

Nano-cathodoluminescence reveals the effect of electron damage on the optical properties of nitride optoelectronics and the damage threshold

James T. Griffiths,¹ Siyuan Zhang,¹ Jeremy Lhuillier,¹ Dandan Zhu,¹ Wai Yuen Fu,² Ashley Howkins,³ Ian Boyd,³ David Stowe,⁴ David J. Wallis,¹ Colin J. Humphreys,¹ and Rachel A. Oliver¹

¹Department of Materials Science and Metallurgy, University of Cambridge, Cambridge CB3 0FS, United Kingdom

²Department of Electrical and Electronic Engineering, The University of Hong Kong, Pokfulam Road, Hong Kong

³Experimental Techniques Centre, Brunel University, Uxbridge UB8 3PH, United Kingdom

⁴Gatan UK, 25 Nuffield Way, Abingdon, Oxon OX14 1RL, United Kingdom

(Received 3 August 2016; accepted 10 October 2016; published online 28 October 2016)

Nano-cathodoluminescence (Nano-CL) reveals optical emission from individual InGaN quantum wells for applications in optoelectronic devices. We show the luminescent intensity decays over time with exposure to the electron beam for energies between 80 and 200 keV. Measurements of the CL intensity over time show an exponential decline in intensity, which we propose is due to the formation of nitrogen Frenkel defects. The measured CL damage decreases with reductions in the electron accelerating voltage and we suggest that the electron induced structural damage may be suppressed below the proposed damage threshold. The electron beam induced damage leads to a non-radiative region that extends over the measured minority carrier diffusion length. Nano-CL may thus serve as a powerful technique to study III-nitride optoelectronics. © 2016 Author(s). All article content, except where otherwise noted, is licensed under a Creative Commons Attribution (CC BY) license (<http://creativecommons.org/licenses/by/4.0/>). [<http://dx.doi.org/10.1063/1.4965989>]

INTRODUCTION

III-nitride white light emitting diodes (LEDs) show superior energy efficiency in contrast to traditional lighting forms, leading to substantial reductions in energy consumption and consequently air pollutants and greenhouse gas emissions.^{1,2} Multiple quantum wells (QW) are often employed to confine the electron and hole wavefunctions, leading to potentially higher radiative recombination rates and device efficiencies. However, there still remains a number of challenges facing the development of nitride optoelectronics, particularly a reduction in the efficiency at higher drive currents for general lighting applications, known commonly as “efficiency droop.”^{3–11} A number of theoretical strategies have been proposed to overcome these challenges, including using QWs with different structural parameters within the same LED.^{12,13} However to assess the success of such approaches requires direct correlation between the structural and optical properties of individual optical nanostructures.

Common approaches though to study the optical properties such as photoluminescence (PL) and electroluminescence (EL), lack the spatial resolution to resolve the emission from individual quantum emitters. Recently however, cathodoluminescence (CL) in a scanning transmission electron microscope (STEM), has been used to show variations in the optical properties of individual GaN quantum disks in nanowires,^{14,15} whilst simultaneously revealing the structural properties, an approach known as nano-cathodoluminescence (nano-CL). Similarly, our own studies have recently revealed quantum confinement effects in individual InGaN QWs in high brightness LEDs.¹⁶ Nano-CL has also been applied to study the nanoscale optical properties of semi-polar InGaN

QWs,¹⁷ GaN nanocolumns,¹⁸ InGaN insertion in in nanowires,¹⁹ and GaN quantum dots.^{20,21}

However, as early as 1990 Yamamoto reported that the luminescent intensity of GaAs quenches under the high energy electron probe, due to the destruction of luminescent centres and the formation of non-radiative defects.²² Electron beam induced damage has similarly been reported in InGaN^{23–27} previously down to an electron energy of 120 keV.²⁸ The interaction between the sample and high energy electrons has been reported to lead to the formation of indium rich clusters,^{29–31} as well as the formation of nitrogen vacancy-interstitials (Frenkel defects).^{32–34} In this study, we investigate the effect of the high energy electron probe on the structure of InGaN QWs and the impact on the luminescent intensity.

METHODS AND MATERIALS

For this study, multiple InGaN quantum wells were grown with gallium nitride barriers by metal organic vapour phase epitaxy. A 200 nm AlN buffer layer was grown on silicon (111) followed by the growth of 600 nm graded AlGaIn and a 1.3 μm non-intentionally doped GaN buffer layer for stress management. A SiN_x interlayer was incorporated to reduce the dislocation density to $\sim 1 \times 10^9 \text{ cm}^{-2}$, and further details on the growth of III-nitrides on silicon can be found in the review by Zhu *et al.*³⁵ Six 3.0 nm thick In_{0.17}Ga_{0.83}N QWs were grown separated by 13.5 nm thick GaN barriers silicon doped at $1 \times 10^{18} \text{ cm}^{-3}$, along with a 13.5 nm GaN capping layer.

Nano-CL experiments were performed on a JEOL 2100 F 80–200 keV Schottky field emission gun TEM fitted with a Gatan Vulcan CL system. Miniature elliptical mirrors

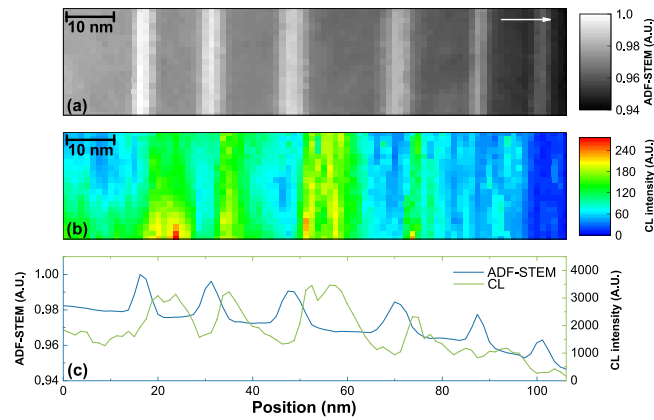


FIG. 1. NanoCL spectrum imaging shows (a) ADF-STEM imaging of the six QWs where the white arrow indicates the growth direction, along with (b) the peak CL intensity of the Gaussian fitted curve showing six distinct optical features corresponding to the QWs. (c) The integrated ADF-STEM and CL intensities, shows the CL intensity peaks at the upper surface of the QWs.

above and below the specimen to provide a light collection angle of up to 7.2 sr. To increase the luminescence, all CL measurements were recorded at 100 K. The samples for STEM were prepared by mechanical polishing followed by precision Ar^+ ion milling at 5 keV, with a final 1 keV polish.

SPECTRAL IMAGING OF InGaN QUANTUM WELLS

Nano-CL spectral imaging is used to reveal the optical characteristics of InGaN/GaN QWs. The spectral image was recorded with a 0.5 nm electron probe and 6.4 pA probe current, over 19×86 1.25 nm pixels, for 0.1 s corresponding to a total current of 1046 pA-s at 80 keV. A Gaussian profile was fitted to the QW peak of the spectrum of each pixel to determine the peak emission intensity. The measured peak QW intensity reveals six high intensity optical features (Figure 1(b)) that correlate directly with the QWs in the corresponding annular dark field (ADF) STEM image (Figure 1(a)) shown with high intensity. The optical features show a spatial separation finer than the QW separation of 16.5 nm. A decrease in the CL intensity of each of the QWs along the growth direction is observed as the specimen thickness decreases indicated by the decrease in the corresponding ADF-STEM intensity. The intensity profiles integrated along the width of the image shown in Figure 1(c), indicates that the peak QW intensity proceeds the ADF-STEM image

along the polar axis. Tizei *et al.* have proposed that electrons and holes drift in opposing directions in response to the internal electric field. Since the emission is dominated by the recombination of the minority carriers (holes) there is likely to be greater emission on the gallium polar side as holes drift towards the quantum well to recombine, in contrast to the opposing side where holes drift away from the quantum well.³⁶

OBSERVATION OF ELECTRON BEAM INDUCED DAMAGE

Whilst nano-CL spectral imaging can provide spectral information with unprecedented insights into the optical properties of individual nanostructures, the exposure to the high energy electron beam used in STEM leads to a reduction in the CL intensity. Figure 2 shows a composite image of the ADF-STEM image and corresponding panchromatic CL image overlaid in blue before (Figure 2(a)) and after (Figure 2(b)) performing a spectral line profile at 80 keV. The difference in the CL images reveals quenching of the luminescent intensity down to 80 keV in the vicinity of the line profile, whilst the ADF-STEM intensity remains constant. The corresponding CL intensity profiles integrated along the growth direction shown in Figure 2(c), reveals the reduction in CL intensity after performing the line profile scan relative to the original image. The electron probe conditions for the line profile were 13.3 pA, over 130 pixels of each 1 nm, recorded for 1 s, corresponding to 1730 pA-s, and hence substantially greater than the spectrum image shown in Figure 1, and further concentrated over just a 130 nm line profile to highlight the effect of the electron probe on the CL intensity. Without the peak fitting previously used the individual QW resolution may not be observed, due to the presence of the defect background signal. The non-radiative region around the line profile scan extends out to a FWHM of ~ 80 nm from where the spectrum line profile was performed despite the sub-nanometre electron probe.

GaN DIFFUSION LENGTH OF MINORITY CARRIERS

Since the electron probe size is negligible with respect to the size of the non-radiative region, the other contribution to the CL spatial distribution arises from the diffusion of carriers. We study the minority carrier diffusion length by scanning the electron probe from the bulk towards the QWs and

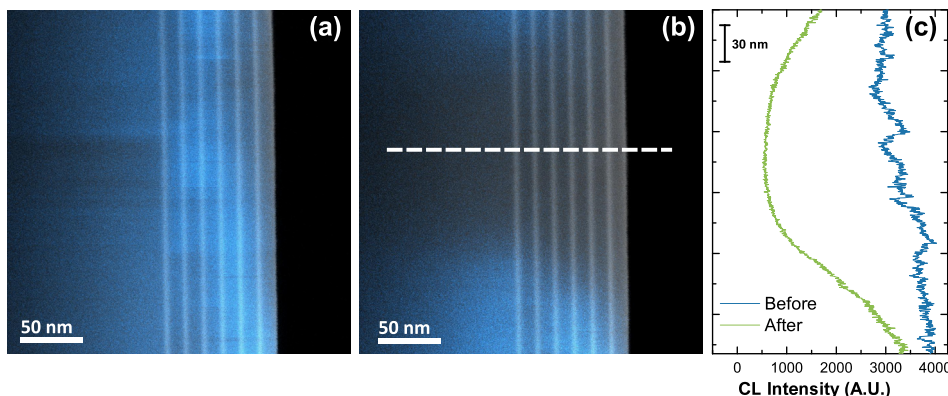


FIG. 2. Composite image of the ADF-STEM image (grayscale) and the panchromatic CL intensity shown in blue at 80 keV (a) before and (b) after a spectral line profile indicated by the dashed white line, along with (c) the CL intensities integrated along growth direction.

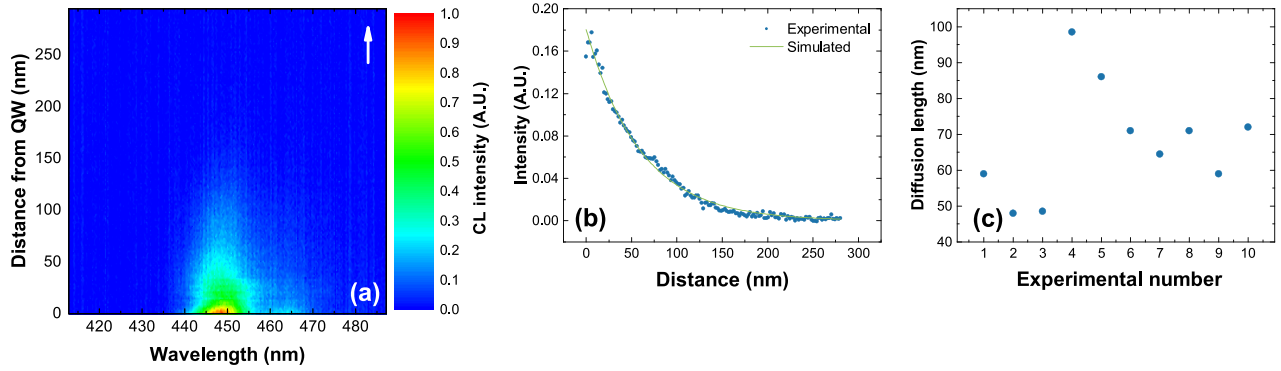


FIG. 3. (a) The variation in the CL spectral intensity as the probe is scanned towards the first QW. The white arrow indicates the direction of the electron line profile. (b) Simulation of the variation in the carrier concentration with respect to the electron probe position with a 60 nm minority carrier diffusion length compared with the experimental measurements. (c) The variation in the measured diffusion length over several measurements.

observe the variation in the luminescence. As the probe is scanned towards the QWs an increase in the luminescent intensity is observed as an increasing number of carriers diffuse to and recombine within the QW as shown in Figure 3(a). The fraction of carriers that can recombine in the QW is directly related to the diffusion length of the carriers. For quantification of the diffusion length the simulated CL intensities may be fitted to the experimental results. For an electron beam with a negligible width compared to the minority carrier diffusion length, the luminescent intensity at the characteristic wavelength of the quantum wells is described by³⁷

$$I(r) = \alpha \int_r^{+\infty} \int_{-\infty}^{+\infty} K_0 \left(\frac{\sqrt{x^2 + y^2}}{L} \right) dy dx, \quad (1)$$

where K_0 is the zero order modified Bessel function of the second kind, L is the minority carrier diffusion length, r denotes the distance between the probe and the QW region, x is the position along the growth axis and y the position perpendicular, and α is the initial CL intensity constant. The experimental carrier concentrations are compared with the simulated minority carrier concentration, which corresponds to the integrand of the previous formula, and an example is shown in Figure 3(b) with a diffusion length of 60 nm. For statistical reliability, the diffusion length was measured by comparing 10 line profiles with the simulated results and the results are shown in Figure 3(c). The average diffusion length measured was 68 nm, with a standard deviation of 15 nm. The measured value is within the range often reported by CL measurements (25–300 nm),^{17,38–46} although there have also been reports of minority carrier diffusion lengths measured by alternate methods, which have been reported to extend to up to several microns.^{47–49} The measured diffusion length is comparable to the observed width of the non-radiative region around the incident electron probe seen in Figure 2 and we propose that the induced defects trap the surrounding carriers.

CL DAMAGE MECHANISM

To investigate the origin of CL quenching, the variation in CL intensity over time was studied by exposing the first QW to the electron probe over electron energies ranging

from 80 to 200 keV. Over all electron energies an immediate exponential decay in the luminescent intensity of the QW emission at 450 nm was observed, shown at 200 keV in Figure 4. Whilst the emission intensity from the QW declines there is no variation in the QW emission wavelength over time.

We quantitatively study the decay in the luminescent signal by recording more than 20 spectral CL time profiles at 80, 100, 120, and 200 keV. We measure the decay lifetime, by fitting an exponential function to each of the spectral CL time profiles. The average CL decay lifetime exhibits an inverse relationship with the accelerating voltage shown in Figure 5, indicating an increasing damage cross section at higher electron beam energies. The increase in damage at higher accelerating voltages suggests that the observed damage is the result of displacement (knock-on) induced damage⁵⁰ as the cross section for ionisation damage decreases with electron beam energy. A linear function fitted to the reciprocal of the damage lifetimes suggests that the damage threshold is 71 ± 5 keV.

The theoretical threshold of electron beam energy to induce displacement damage depends on the atomic weight ($N=14$, $Ga=69$) M, and the required minimum energy transfer to break the bonds E_d , which is given by⁵⁰

$$E_{threshold} = mc^2 \left(\sqrt{\frac{ME_d}{2m^2c^2} + 1} - 1 \right), \quad (2)$$

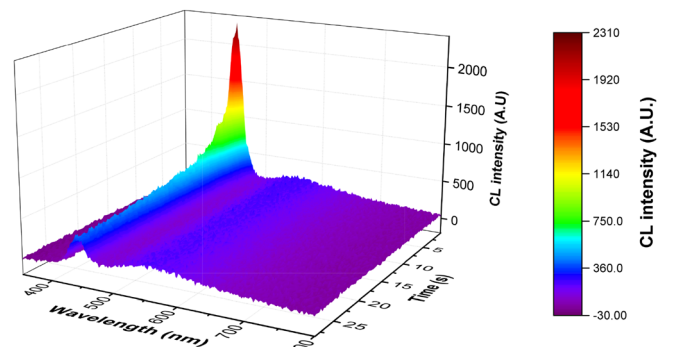


FIG. 4. Variation in the CL intensity with time shows an exponential decline in the luminescent intensity, with no variation in emission wavelength, measured at 200 keV.

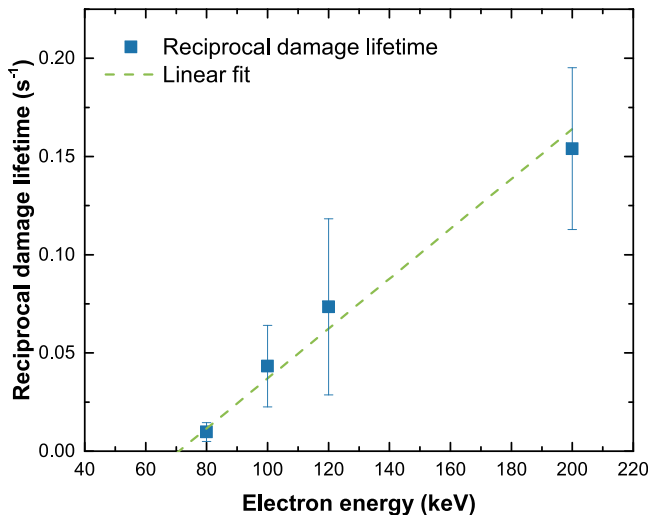


FIG. 5. The variation in the reciprocal CL lifetime with respect to the accelerating voltage. A linear fit shows an intercept at 71 keV, suggesting a threshold for electron beam induced damage.

where m is the electron mass, c is the speed of light. The minimum energy transfer to generate a N interstitial-vacancy pair (Frenkel defect) has been calculated to be 17 eV, and for a Ga Frenkel defect, 39 eV,⁵¹ corresponding to a threshold electron energy of 100 keV and 729 keV, respectively, in GaN. Due to the lower cohesive binding energy in InN⁵² the threshold may be lower in InGaN. The observed damage threshold, suggests the generation of N Frenkel defects is the dominant factor in the reduction of the CL intensity. Nitrogen vacancies are reported to introduce an additional shallow state below the conduction band,^{33,53,54} leading to non-radiative recombination and the observed quenching of the emission. There may also be a contribution to the reduction in the CL intensity below the predicted threshold from sputtering from surfaces or ionisation damage though further CL experiments at lower electron energies may help to reveal further insights into the damage process.

CONCLUSION

We have shown that electron beam induced damage may be minimised by reducing the electron beam energy, and nano-CL can reveal the optical properties of individual InGaN QWs for high brightness optoelectronic devices. The CL intensity was shown to exhibit an exponential decline with exposure to the electron beam over electron energies ranging from 80 to 200 keV. The measured decay CL lifetimes indicate that the damage is substantially reduced at lower accelerating voltages and we propose that below the energy threshold, damage free imaging is possible. The electron beam is proposed to lead to the formation of nitrogen vacancies, which act as shallow non-radiative potential centres and quench the emission over an area corresponding to the minority carrier diffusion length. Nano-CL may therefore serve as a reliable experimental approach to the simultaneous study of the optical and structural properties with nanoscale resolution of III-nitride optoelectronic devices.

ACKNOWLEDGMENTS

This work was carried out with the support of the United Kingdom Engineering and Physical Sciences Research Council under Grant Nos. EP/NO17927/1 and EP/J003603/1. R. Oliver acknowledges funding from the European Research Council under the European Community's Seventh Framework Programme (FP7/2007-2013) ERC grant agreement number 279361 (MACONS) and the from the Royal Academy of Engineers/Leverhulme Trust senior research fellowship. This research is conducted in part using the research computing facilities offered by Information Technology Services at the University of Hong Kong. Data used in this publication may be accessed at the following link <http://dx.doi.org/10.17863/CAM.6009>.

- ¹C. J. Humphreys, *MRS Bull.* **33**, 459 (2008).
- ²S. Nakamura, *Rev. Mod. Phys.* **87**, 1139 (2015).
- ³J. Iveland, L. Martinelli, J. Peretti, J. S. Speck, and C. Weisbuch, *Phys. Rev. Lett.* **110**, 177406 (2013).
- ⁴Y. C. Shen, G. O. Mueller, S. Watanabe, N. F. Gardner, A. Munkholm, and M. R. Krames, *Appl. Phys. Lett.* **91**, 141101 (2007).
- ⁵J. Hader, J. V. Moloney, B. Pasenow, S. W. Koch, M. Sabathil, N. Linder, and S. Lutgen, *Appl. Phys. Lett.* **92**, 261103 (2008).
- ⁶E. Kioupakis, P. Rinke, K. T. Delaney, and C. G. Van de Walle, *Appl. Phys. Lett.* **98**, 161107 (2011).
- ⁷S. Hammersley, D. Watson-Parris, P. Dawson, M. J. Godfrey, T. J. Badcock, M. J. Kappers, C. McAleese, R. A. Oliver, and C. J. Humphreys, *J. Appl. Phys.* **111**, 083512 (2012).
- ⁸M.-H. Kim, M. F. Schubert, Q. Dai, J. K. Kim, E. F. Schubert, J. Piprek, and Y. Park, *Appl. Phys. Lett.* **91**, 183507 (2007).
- ⁹H. Zhao, G. Liu, R. A. Arif, and N. Tansu, *Solid. State. Electron.* **54**, 1119 (2010).
- ¹⁰J. Piprek, *Phys. Status Solidi* **207**, 2217 (2010).
- ¹¹G. Pozina, R. Ciechonski, Z. Bi, L. Samuelson, and B. Monemar, *Appl. Phys. Lett.* **107**, 251106 (2015).
- ¹²D. Y. Kim, G.-B. Lin, S. Hwang, J. H. Park, D. Meyaard, E. F. Schubert, H.-Y. Ryu, and J. K. Kim, *IEEE Photonics J.* **7**, 1 (2015).
- ¹³B. Rouet-Leduc, K. Barros, T. Lookman, and C. J. Humphreys, *Sci. Rep.* **6**, 24862 (2016).
- ¹⁴L. F. Zagonel, S. Mazzucco, M. Tencé, K. March, R. Bernard, B. Laslier, G. Jacopin, M. Tchernycheva, L. Rigutti, F. H. Julien, R. Songmuang, and M. Kociak, *Nano Lett.* **11**, 568 (2011).
- ¹⁵L. F. Zagonel, L. Rigutti, M. Tchernycheva, G. Jacopin, R. Songmuang, and M. Kociak, *Nanotechnology* **23**, 455205 (2012).
- ¹⁶J. T. Griffiths, S. Zhang, B. Rouet-Leduc, W. Y. Fu, A. Bao, D. Zhu, D. J. Wallis, A. Howkins, I. Boyd, D. Stowe, M. J. Kappers, C. J. Humphreys, and R. A. Oliver, *Nano Lett.* **15**, 7639 (2015).
- ¹⁷M. Müller, G. Schmidt, S. Metzner, P. Veit, F. Bertram, R. A. R. Leute, D. Heinz, J. Wang, T. Meisch, F. Scholz, and J. Christen, *Phys. Status Solidi* **253**, 112 (2016).
- ¹⁸A. Urban, M. Müller, C. Karbaum, G. Schmidt, P. Veit, J. Malindretos, F. Bertram, J. Christen, and A. Rizzi, *Nano Lett.* **15**, 5105 (2015).
- ¹⁹X. Zhou, M.-Y. Lu, Y.-J. Lu, E. J. Jones, S. Gwo, and S. Gradečak, *ACS Nano* **9**, 2868 (2015).
- ²⁰G. Schmidt, M. Müller, F. Bertram, P. Veit, S. Petzold, A. Das, and E. Monroy, *Microsc. Microanal.* **18**, 1878 (2012).
- ²¹G. Schmidt, P. Veit, C. Berger, F. Bertram, A. Dadgar, A. Strittmatter, and J. Christen, *Jpn. J. Appl. Phys., Part 1* **55**, 05FF04 (2016).
- ²²N. Yamamoto, *Mater. Trans. JIM* **31**, 659 (1990).
- ²³T. M. Smeeton, M. J. Kappers, J. S. Barnard, M. E. Vickers, and C. J. Humphreys, *Appl. Phys. Lett.* **83**, 5419 (2003).
- ²⁴M. Ishimaru, *Appl. Phys. Lett.* **96**, 191908 (2010).
- ²⁵C. J. Humphreys, *Philos. Mag.* **87**, 1971 (2007).
- ²⁶N. M. Boyall, K. Durose, and I. M. Watson, *Mater. Res. Soc. Symp. Proc.*, 2002, Vol. 743, p. L11.13, available at <http://dx.doi.org/10.1557/PROC-743-L11.13>.
- ²⁷Y. Ohno, Y. Kawai, and S. Takeda, *Phys. Rev. B* **59**, 2694 (1999).
- ²⁸K. H. Baloch, A. C. Johnston-Peck, K. Kisslinger, E. A. Stach, and S. Gradečak, *Appl. Phys. Lett.* **102**, 191910 (2013).

- ²⁹J. P. O'Neill, I. M. Ross, A. G. Cullis, T. Wang, and P. J. Parbrook, *Appl. Phys. Lett.* **83**, 1965 (2003).
- ³⁰T. Li, E. Hahn, D. Gerthsen, A. Rosenauer, A. Strittmatter, L. Reißmann, and D. Bimberg, *Appl. Phys. Lett.* **86**, 241911 (2005).
- ³¹S. E. Bennett, D. W. Saxey, M. J. Kappers, J. S. Barnard, C. J. Humphreys, G. D. Smith, and R. A. Oliver, *Appl. Phys. Lett.* **99**, 021906 (2011).
- ³²M. Petravic, P. N. K. Deenapanray, M. D. Fraser, A. V. Soldatov, Y.-W. Yang, P. A. Anderson, and S. M. Durbin, *J. Phys. Chem. B* **110**, 2984 (2006).
- ³³D. C. Look, G. C. Farlow, P. J. Drevinsky, D. F. Bliss, and J. R. Sizelove, *Appl. Phys. Lett.* **83**, 3525 (2003).
- ³⁴D. C. Look, D. C. Reynolds, J. W. Hemsley, J. R. Sizelove, R. L. Jones, and R. J. Molnar, *Phys. Rev. Lett.* **79**, 2273 (1997).
- ³⁵D. Zhu, D. J. Wallis, and C. J. Humphreys, *Rep. Prog. Phys.* **76**, 106501 (2013).
- ³⁶L. H. G. Tizei, S. Meuret, K. March, K. Hestroffer, T. Auzelle, B. Daudin, and M. Kociak, *Appl. Phys. Lett.* **105**, 143106 (2014).
- ³⁷M. Lax, *J. Appl. Phys.* **49**, 2796 (1978).
- ³⁸N. Yamamoto, H. Itoh, V. Grillo, S. F. Chichibu, S. Keller, J. S. Speck, S. P. DenBaars, U. K. Mishra, S. Nakamura, and G. Salviati, *J. Appl. Phys.* **94**, 4315 (2003).
- ³⁹N. Ino and N. Yamamoto, *Appl. Phys. Lett.* **93**, 232103 (2008).
- ⁴⁰S. J. Rosner, E. C. Carr, M. J. Ludowise, G. Girolami, and H. I. Erikson, *Appl. Phys. Lett.* **70**, 420 (1997).
- ⁴¹P. M. Bridger, Z. Z. Bandić, E. C. Piquette, and T. C. McGill, *Appl. Phys. Lett.* **73**, 3438 (1998).
- ⁴²T. M. Levin, G. H. Jessen, F. A. Ponce, and L. J. Brillson, *J. Vac. Sci. Technol. B: Microelectron. Nanometer Struct.* **17**, 2545 (1999).
- ⁴³S. Chichibu, K. Wada, and S. Nakamura, *Appl. Phys. Lett.* **71**, 2346 (1997).
- ⁴⁴P. Hacke, A. Kuramata, K. Domen, K. Horino, and T. Tanahashi, *Phys. Status Solidi* **216**, 639 (1999).
- ⁴⁵D. Cherns, S. J. Henley, and F. A. Ponce, *Appl. Phys. Lett.* **78**, 2691 (2001).
- ⁴⁶H. Takahashi, A. Ito, T. Tanaka, A. Watanabe, H. Ota, and K. Chikuma, *Jpn. J. Appl. Phys., Part 2* **39**, L569 (2000).
- ⁴⁷J. C. Gonzalez, K. L. Bunker, and P. E. Russell, *Appl. Phys. Lett.* **79**, 1567 (2001).
- ⁴⁸L. Chernyak, A. Osinsky, and A. Schulte, *Solid State Electron.* **45**, 1687 (2001).
- ⁴⁹A. Cremades, M. Albrecht, J. Krinke, R. Dimitrov, M. Stutzmann, and H. P. Strunk, *J. Appl. Phys.* **87**, 2357 (2000).
- ⁵⁰R. F. Egerton, R. McLeod, F. Wang, and M. Malac, *Ultramicroscopy* **110**, 991 (2010).
- ⁵¹H. Y. Xiao, F. Gao, X. T. Zu, and W. J. Weber, *J. Appl. Phys.* **105**, 123527 (2009).
- ⁵²C. Stampfl and C. G. Van De Walle, *Phys. Rev. B* **59**, 5521 (1999).
- ⁵³J. Buckeridge, C. R. A. Catlow, D. O. Scanlon, T. W. Keal, P. Sherwood, M. Miskufova, A. Walsh, S. M. Woodley, and A. A. Sokol, *Phys. Rev. Lett.* **114**, 016405 (2015).
- ⁵⁴P. Boguslawski, E. L. Briggs, and J. Bernholc, *Phys. Rev. B* **51**, 17255 (1995).